

Anomalous temperature dependent heat transport in one-dimensional momentum-conserving systems with soft-type interparticle interaction

Daxing Xiong*

Department of Physics, Fuzhou University, Fuzhou 350108, Fujian, China

To date, most of the theoretical and numerical studies on heat transport are only focused on the systems whose interparticle interactions are usually Fermi-Pasta-Ulam (FPU) like and hard-type (HT). Here we investigate how the transport behavior would be changed when the soft-type (ST) interaction is considered. We find that with the increase of system's temperature, introducing the ST interaction softens phonons and decreases their velocities, while this type of nonlinearity, similarly to its counterpart of HT, cannot fully damp the longest wave phonons. Therefore, an anomalous temperature dependent heat transport with certain scaling behavior similarly to those in the FPU-like systems with HT interactions can be seen. Our detailed examination from simulations well verify this temperature dependent behavior.

I. INTRODUCTION

As one of the fundamental topics closely related to the concepts of nonlinearity and irreversibility in statistical mechanics [1], heat transport in one-dimensional (1D) systems has attracted considerable interest in recent years [2–5]. In this context, one of the central issues is the validity or breakdown of Fourier's law, which states, the heat flux \mathbf{J} is proportional to the temperature gradient ∇T : $\mathbf{J} = -\kappa \nabla T$, with κ the heat conductivity assumed to be a size-independent constant. Generally, it is now well accepted that for 1D anharmonic systems with conserved momentum, the Fourier's law is not valid, namely κ is not a constant but diverges with the system size L in a power law $\kappa \sim L^\alpha$ [2, 3, 6–11]. The exponent α ($0 \leq \alpha \leq 1$) is believed to follow some universality classes [2, 3, 7–9, 11–16], which was supported by some theories [8, 9, 12–16] and numerical simulations [7, 11, 17, 18], and debated by some other studies [19–25]. While it should be noted that if some other factors, like the asymmetric interactions [26–30], the systems close to the integrable limit [31], the pressure [32, 33], and the multi-well interparticle potential [34–40], are included, whether the Fourier's law is still valid/invalid and what are the underlying mechanics, the verification remains in progress.

It is thus necessary to check the heat transport behavior including more complicated factors to seek general conclusions. In the present work we therefore consider a momentum-conserving system with the soft-type (ST) interparticle interaction, which is a new factor that has not yet been fully taken into account [compared with the hard-type (HT) interactions]. Our main finding is that, similar to the Fermi-Pasta-Ulam- β (FPU- β) systems with the HT anharmonicity, an anomalous heat transport will be seen at all temperatures. Via detailed simulations we also explore the possible microscopic mechanism. We show that with the increase of

the system's temperature, the ST interaction induces a special type of nonlinearity, which softens the phonons and reduces their velocities; while these effects cannot qualitatively change the heat transport and its scaling behavior. A careful analysis of the system's momentum spread and phonon spectra indicates an incomplete damping process of phonons very similarly to those exhibited in FPU- β systems with HT anharmonicity. This may be the reason for the anomalous temperature dependent heat transport behavior observed here.

The rest of this work is organized as follows: In Sec. II we introduce the model and compare the ST anharmonic interaction with the potentials of Harmonic and FPU- β (with HT interaction) systems. Section III describes the simulation method. We use the equilibrium correlation simulation method [41, 42] to get the heat spreading information with the temperatures, from which our main results on heat transport and its scaling property are presented in Sec. IV. Section V is devoted to the underlying mechanisms. For such purpose we investigate the system's momentum spread and examine the phonons spectra to explore the phonons' damping information. Finally, a summary is given in Sec. VI.

II. MODEL

We consider a 1D many-particle (L particles) momentum-conserving lattice with Hamiltonian

$$H = \sum_{m=1}^L p_m^2/2 + V(r_{k+1} - r_k), \quad (1)$$

where p_k is the k -th particle's momentum and r_k its displacement from equilibrium position. The interparticle potential takes a type of soft anharmonicity [43–45]

$$V(\xi) = |\xi| - \ln(1 + |\xi|), \quad (2)$$

which is shown in Fig. 1(a) and also compared with the Harmonic [$V(\xi) = \xi^2/2$] and FPU- β [$V(\xi) = \xi^2/2 + \xi^4/4$] potentials.

*Electronic address: phyxiongdx@fzu.edu.cn

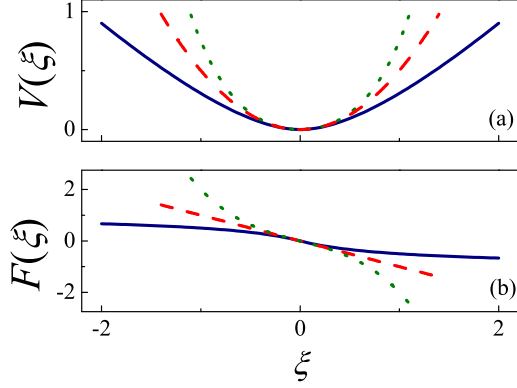


FIG. 1: (Color online) The ST anharmonic interparticle potential [Eq. (2), solid] (a) and its associated force (b). For comparison we also plot the counterparts of Harmonic (dashed) and FPU- β (dotted) systems.

Figure 1(b) plots the associated forces defined by $F(\xi) = -\partial V(\xi)/\partial \xi$. As can be seen, opposite to the FPU- β system with HT anharmonicity, the ST interaction has a restoring force always less than the Harmonic force. This is why we call it ST anharmonicity, a special feature of the system. It induces an unusual energy dependent frequency [43], which has been suggested to strongly modify the distribution, intensity, and mobility of the thermal fluctuations, resulting in a quite different transition dynamics of the underlying activated process [45]. With this model here we aim to explore how this ST anharmonicity would play the roles in heat transport.

III. METHOD

As mentioned, to identify the heat transport behavior and its scaling property, we here use the equilibrium correlation method [41, 42]. For the special ST anharmonicity, it can be expected that the time scale to ensure the system relaxed to the nonequilibrium stationary state would be quite longer than the usually considered FPU- β systems with HT anharmonicity. This would be why the traditional simulation methods, such as the direct nonequilibrium molecular dynamics simulations [6] and the approach based on the Green-Kubo formula [8] have not yet been used to study such a system, and thus the heat transport law here is still unclear.

The equilibrium correlation method [41, 42] employs the following normalized spatiotemporal correlation function of system's heat energy fluctuations to explore the heat spreading information

$$\rho_Q(m, t) = \frac{\langle \Delta Q_j(t) \Delta Q_i(0) \rangle}{\langle \Delta Q_i(0) \Delta Q_i(0) \rangle}, \quad (3)$$

where $m = j - i$; $\langle \cdot \rangle$ represents the spatiotemporal average; $\Delta Q_i(t) \equiv Q_i(t) - \langle Q_i \rangle$ is the heat energy $Q_i(t)$'s

fluctuation in an equal and appropriate lattice bin i (the number of particles in the i -th bin is equal to $N_i = L/b$, where b is the total number of the bins). In each bin, $Q_i(t) \equiv \sum Q(x, t)$ with $Q(x, t) \equiv E(x, t) - \frac{(\langle E \rangle + \langle F \rangle)M(x, t)}{\langle M \rangle}$ [46, 47] the single particle's heat energy density at the absolute space x and time t within the bin, which is closely related to the corresponding energy (mass) density $E(M)$ under a internal average pressure $\langle F \rangle$.

In order to understand the underlying picture, we also study the momentum spread via the momentum correlation function

$$\rho_p(m, t) = \frac{\langle \Delta p_j(t) \Delta p_i(0) \rangle}{\langle \Delta p_i(0) \Delta p_i(0) \rangle}. \quad (4)$$

Similarly to the definition of $\rho_Q(m, t)$, here $\Delta p_i(t) \equiv p_i(t) - \langle p_i \rangle$ denotes the momentum fluctuation.

To calculate the correlation functions, the system is first thermalized to the focused temperature by using the stochastic Langevin heat baths [2, 3] for a long enough time ($> 10^7$ time units of the models). This should be taken from properly assigned initial random states. Then the system is evolved in isolation [by using the Runge-Kutta algorithm of 7th to 8th order with a time step 0.05] for deriving the correlation information. We use the size of ensemble about 8×10^9 .

We consider a wide range of temperatures from $T = 0.00075$ to $T = 0.75$. For each temperature, we set the chain size of $L = 2001$, which allows a fluctuation of heat located at the center to spread along the system for a long time at least up to $t = 600$. Under this setup, we apply the periodic boundary conditions, fix the bins number $b \equiv L/2$ (the choice of b has been verified not to affect the final results).

IV. HEAT SPREADING AND ITS SCALING

Now let us see the results of heat spread. In Fig. 2 we first plot the profiles of $\rho_Q(m, t)$ for typical three long time. Four temperatures T , from low to high, are employed to explore the temperature dependent behavior. As can be seen, with the increase of T , the profile of $\rho_Q(m, t)$ is changed from a U shape [48] to Lévy walks [14, 15] density, especially that the central parts of the profile become more and more localized. The U shape here shows slight difference with the usual density in Harmonic chain, i.e., the front parts exhibit some oscillations, which may be caused by the unusual non-linearity of ST anharmonicity under low temperatures. The Lévy walks profiles under high temperatures can be phenomenologically understood from the single particle Lévy walks theory with velocity fluctuations [49].

The scaling analysis of $\rho_Q(m, t)$ is usually focused on the central parts by using the following formula

$$t^{1/\gamma} \rho_Q(m, t) \simeq \rho_Q\left(\frac{m}{t^{1/\gamma}}, t\right). \quad (5)$$

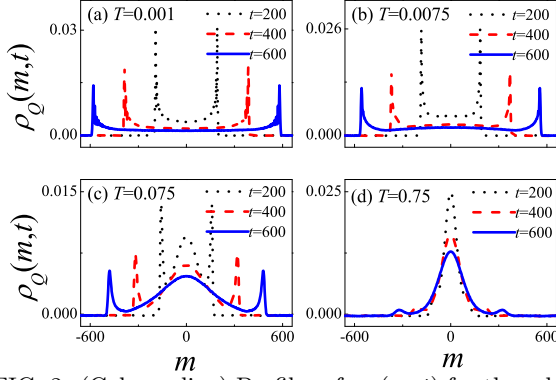


FIG. 2: (Color online) Profiles of $\rho_Q(m, t)$ for three long time $t = 200$ (dot), $t = 400$ (dash) and $t = 600$ (solid) under temperatures $T = 0.001$ (a); $T = 0.0075$ (b); $T = 0.075$ (c) and $T = 0.75$ (d), respectively.

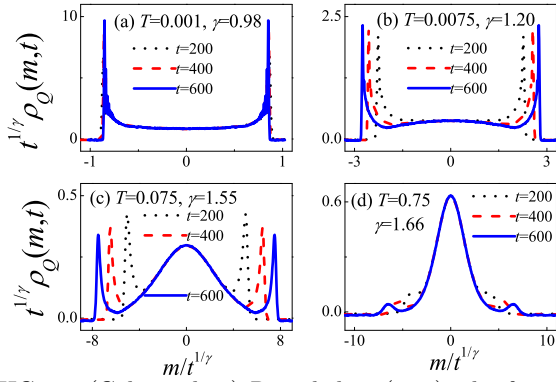


FIG. 3: (Color online) Rescaled $\rho_Q(m, t)$, the focused temperatures here are the same as those in Fig. 2.

We then use formula (5) to rescale the profiles as shown in Fig. 2, which enables us to identify a scaling exponent γ for characterizing the heat spreading's scaling behavior. We recall here $\gamma = 1$ and $1 < \gamma < 2$ correspond to ballistic and super-diffusive heat transport, respectively. Now it is clear that the U shape shown at low temperatures [$\gamma = 0.98$ close to 1, see Fig. 3(a)] indicates the ballistic heat transport, while the Lévy walks density under high temperatures implies the super-diffusive behavior [Fig. 3(d), $\gamma = 1.66 > 1$]. For the ballistic regime the whole density can be perfectly scaled by formula (5), both for central and front parts, while in the super-diffusive case, only the central parts are available, which might correspond to the bi-linear scaling property of Lévy walks [50].

The scaling exponent γ is of great interest since from which we might get the time scaling exponent of the mean squared deviation of this heat diffusion process and thus connect to the divergence exponent α of heat transport [51, 52]. Figure 4 depicts γ versus temperature T . Therein four data points are extracted from Fig. 3, others are obtained by performing the same scaling analysis. The results clearly indicate the temperature dependent γ exponents though it was usually suggested that γ

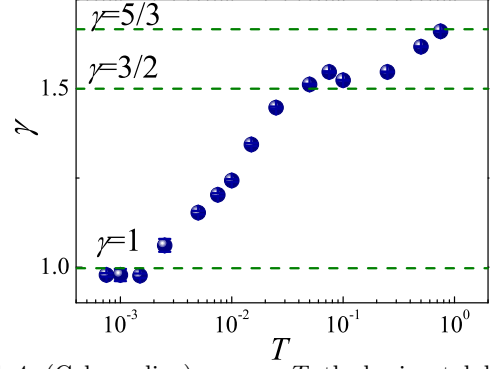


FIG. 4: (Color online) γ versus T , the horizontal dashed lines, from bottom to top, denote $\gamma = 1$, $\gamma = 3/2$ and $\gamma = 5/3$, respectively.

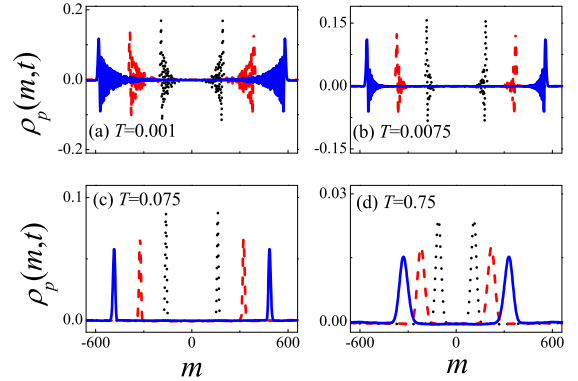


FIG. 5: (Color online) Momentum spread $\rho_p(m, t)$ for three long time $t = 200$ (dot), $t = 400$ (dash) and $t = 600$ (solid) under temperatures $T = 0.001$ (a); $T = 0.0075$ (b); $T = 0.075$ (c) and $T = 0.75$ (d), respectively.

should follow two universality classes, i.e., $\gamma = 3/2$ and $\gamma = 5/3$ predicted by some theories [13]. Interestingly such anomalous temperature dependent behavior is similar to that shown in FPU- β chain [39], where the nonlinearity dependent γ exponents crossover between different universality classes have been reported.

V. UNDERLYING MECHANISM

Why can we see such anomalous temperature dependent heat transport? Is there any new properties after including the ST anharmonic interaction? To answer these questions, we here first study the momentum spread and then explore the properties of phonons' damping with the temperatures.

A. Momentum spread

Figure 5 depicts the results of momentum spread $\rho_p(m, t)$. As for comparison, three long time and four typical temperatures, the same as those in heat spread

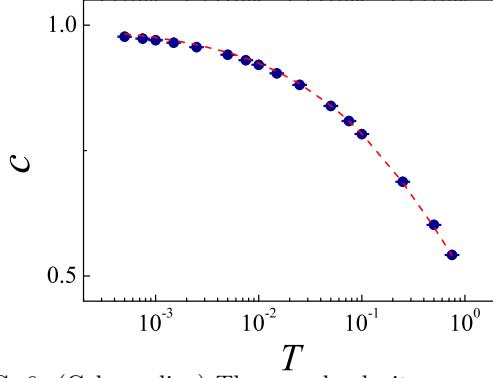


FIG. 6: (Color online) The sound velocity c versus T , where the dashed line denotes the predictions from formula (6).

are considered. As can be seen, the momentum spread also indicates interesting temperature dependent behavior: while at low temperatures there are some oscillations in the profiles of $\rho_p(m, t)$ [see Fig. 5(a)]; with the increase of T , such oscillations become less and less [see Fig. 5(b)], and eventually disappear [see Fig. 5(c)]; after that if one increases the temperature further, the front peaks begin to disperse [see Fig. 5(d)]. Thus this unusual change of $\rho_p(m, t)$ with temperatures may correspond to the anomalous temperature dependence of heat spread.

It was usually suggested that the velocity of the front peaks shown in the momentum spread just corresponds to the sound velocity c [53]. A recent theory [13] proposed a general formula

$$c = \sqrt{\frac{\frac{1}{2}T^2 + \langle V + \langle F \rangle \xi; V + \langle F \rangle \xi \rangle}{\frac{1}{T} \left(\langle \xi; \xi \rangle \langle V; V \rangle - \langle \xi; V \rangle^2 \right) + \frac{1}{2}T \langle \xi; \xi \rangle}} \quad (6)$$

which can predict the sound velocity for systems with any interparticle interaction. In formula (6), $V(\xi)$ is the interparticle potential, $\langle A; B \rangle$ denotes the covariance $\langle AB \rangle - \langle A \rangle \langle B \rangle$ for any two quantities A and B , $\langle F \rangle$ is the averaged pressure ($\langle F \rangle \equiv 0$ for symmetric potentials). It is thus worthwhile to check whether formula (6) is still valid here. For such purpose, we numerically measure the velocity of front peaks as shown in $\rho_p(m, t)$ for each temperature and compare the result with the prediction from formula (6). To obtain the theoretical predictions, we insert the ST anharmonic potential [Eq. (2)] into formula (6) and calculate the ensemble average of each quantity $\langle A \rangle$ by $\int_{-\infty}^{\infty} A e^{-V(\xi)/T} d\xi / \int_{-\infty}^{\infty} e^{-V(\xi)/T} d\xi$.

Figure 6 shows the result of c versus T . As can be seen, the numerical measurements match the predictions quite well, suggesting that indeed, the formula (6) can also be validated to the systems with ST anharmonicity. More-importantly, both results indicate the decrease of sound velocity with temperatures, which is clearly opposite to the results as shown in the FPU- β chain [53]. Thus, this may be a general feature for systems with ST anharmonicity.

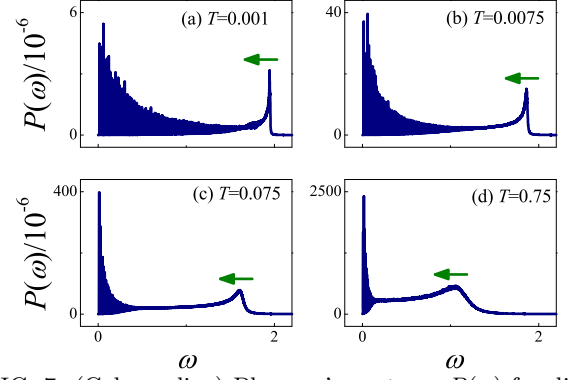


FIG. 7: (Color online) Phonons' spectrum $P(\omega)$ for different temperatures: (a) $T = 0.001$; (b) $T = 0.0075$; (c) $T = 0.075$; (d) $T = 0.75$, respectively.

B. Phonon spectrum

Clearly, the decrease of sound velocity cannot be used to fully understand the temperature dependence of heat spread. We thus turn to analyze how the phonon spectrum $P(\omega)$ would depend on temperature, from which one may gain further useful information, since a quite recent work [40] suggested that both phonons' damping and softening are crucial to the observed normal heat transport ($\alpha = 0$, satisfy the Fourier's law).

The phonon spectra $P(\omega)$ is calculated by applying a frequency ω analysis of the particles' velocity $v(t)$

$$P(\omega) = \lim_{\tau \rightarrow \infty} \frac{1}{\tau} \int_0^\tau v(t) \exp(-i\omega t) dt. \quad (7)$$

To relate to the heat spread, this should be done at the corresponding equilibrium states under the same focused temperature. For facilitating the computation, here we choose a chain of $N = 200$ particles, then thermalize the chain to the focused temperature by Langevin heat baths [2, 3], finally remove the heat baths and perform a frequency analysis of $v(t)$ following Eq. (7). This should also be done by starting from properly assigned initial random states for several times.

Figures 7 and 8 depict the phonons' spectrum $P(\omega)$ for different temperatures. Two key points can be revealed from the results. First, with the increase of temperature, phonons tend to become "softer" since $P(\omega)$ walks towards the direction of low frequency. This can be captured from the locations of the peaks in the high frequency parts (see Fig. 7). To more clearly characterize this phonons softening process, one can measure the averaged frequency $\bar{\omega}$ of phonons by defining $\bar{\omega} = \int_0^\infty P(\omega) \omega d\omega / \int_0^\infty P(\omega) d\omega$. As complementary we plot $\bar{\omega}$ versus T in Fig. 9, from which a monotonous decrease of $\bar{\omega}$ different from the non-monotonous case as shown in [40] can be clearly seen. This seems to suggest that a monotonous phonons softening process is inadequate to induce a normal heat transport.

Let us finally turn to the results of phonons' damping.

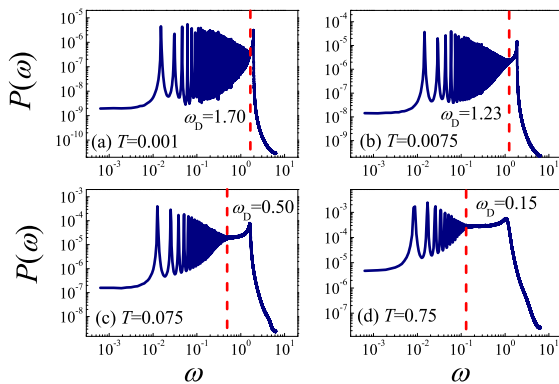


FIG. 8: (Color online) A log-log plot of Fig. 7, where the dotted lines denote the frequencies ω_D below which phonons are damped very weakly.

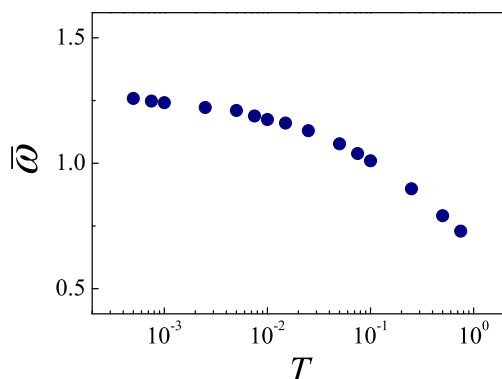


FIG. 9: (Color online) The averaged frequency $\bar{\omega}$ of phonons shown in $P(\omega)$ versus temperature.

Since if it is still called phonon, in its power spectrum at corresponding frequencies there should be some oscillations. With this in mind we then can employ Fig. 8 to observe this phonons' damping process. As can be seen, with the increase of temperature, the damping first originates from the high frequency parts [see Fig. 8(a) and (b)] and then quickly towards the low ones [see Fig. 8(c)]. However, this quick damping process cannot last

forever if one further increases the temperature [see Fig. 8(d)], eventually, a power spectrum of phonons very similar to that shown in FPU- β systems with HT anharmonicity (in the high nonlinearity regime) [39] can be seen. Here we use the critical frequency of ω_D (below which phonons are damped very weakly) to characterize this phonons' damping process. It is worthwhile to note that this incomplete damping process may correspond to the Lévy walks densities observed in heat spread under high temperatures. It also suggests that both ST and HT anharmonicity can only lead to an incomplete damping of phonons, thus generally a universal anomalous heat transport with certain scaling exponents could be seen in nonlinear systems with only ST or HT anharmonicity.

VI. SUMMARY

In summary, we have studied the temperature dependent heat transport behavior in a 1D system when the ST interparticle interaction is considered. We have found that by increasing the temperature, including the ST anharmonicity can induce some opposite effects to the counterpart systems with HT anharmonicity, such as that *monotonously* softening the phonons and decreasing the sound velocity. However, these unusual properties are still inadequate to lead to a normal heat transport. A analysis of phonons spectra indicates an incomplete damping of phonons, especially those at low frequencies. This property of spectra is similar to that shown in the FPU- β system with HT anharmonicity. Our results thus suggest that both ST and HT anharmonicity will eventually lead to a general super-diffusive heat transport behavior, therefore further supporting the conjecture that nonlinearity/chaos is, neither a sufficient nor a necessary condition for the validity of Fourier's law.

Acknowledgments

This work was supported by the NNSF (Grant No. 11575046) of China.

-
- [1] J. P. Francoise, G. L. Naber, and T. S. Tsun, *Encyclopedia of Mathematical physics: Equilibrium Statistical Mechanics; Nonequilibrium Statistical Mechanics* (Science Press, Beijing, China, 2008).
 - [2] S. Lepri, R. Livi, and A. Politi, *Phys. Rep.* **377**, 1 (2003).
 - [3] A. Dhar, *Adv. Phys.* **57**, 457 (2008).
 - [4] S. Lepri, R. Livi, and A. Politi, *Thermal Transport in Low Dimensions*, Lecture Notes in Physics Vol. 921 (Springer, Berlin, 2016).
 - [5] J. Lebowitz, S. Olla, and G. Stoltz, Final report of workshop *Nonequilibrium statistical mechanics: mathematical understanding and numerical simulation* www.birs.ca/events/2012/5-day-workshops/12w5013 (2013).
 - [6] S. Lepri, R. Livi, and A. Politi, *Phys. Rev. Lett.* **78**, 1896 (1997).
 - [7] P. Grassberger, W. Nadler, and L. Yang, *Phys. Rev. Lett.* **89**, 180601 (2002).
 - [8] O. Narayan and S. Ramaswamy, *Phys. Rev. Lett.* **89**, 200601 (2002).
 - [9] G. Basile, C. Bernardin, and S. Olla, *Phys. Rev. Lett.* **96**, 204303 (2006).
 - [10] P. Di Cintio, R. Livi, H. Bufferand, G. Ciraolo, S. Lepri, and M. J. Straka, *Phys. Rev. E* **92**, 062108 (2015).
 - [11] T. Mai, A. Dhar, and O. Narayan, *Phys. Rev. Lett.* **98**, 184301 (2007).
 - [12] H. van Beijeren, *Phys. Rev. Lett.* **108**, 180601 (2012).
 - [13] C. B. Mendl and H. Spohn, *Phys. Rev. Lett.* **111**, 230601 (2013).

- (2013); H. Spohn, J. Stat. Phys. **154**, 1191 (2014).
- [14] V. Zaburdaev, S. Denisov, and J. Klafter, Rev. Mod. Phys. **87**, 483 (2015).
 - [15] V. Zaburdaev, S. Denisov, and P. Hänggi, Phys. Rev. Lett. **106**, 180601 (2011).
 - [16] V. Popkov, A. Schadschneider, J. Schmidt and G. M. Schütz, Proc. Natl. Acad. Sci. U. S. A. **112**, 41 (2015).
 - [17] S. G. Das, A. Dhar, K. Saito, C. B. Mendl, and H. Spohn, Phys. Rev. E **90**, 012124 (2014).
 - [18] C. B. Mendl and H. Spohn, Phys. Rev. E **90**, 012147 (2014).
 - [19] D. Xiong, J. Wang, Y. Zhang, and H. Zhao, Phys. Rev. E **85**, 020102 (R) (2012).
 - [20] D. Xiong, Y. Zhang, and H. Zhao, Phys. Rev. E **88**, 052128 (2013).
 - [21] D. Xiong, Y. Zhang, and H. Zhao, Phys. Rev. E **90**, 022117 (2014).
 - [22] G. R. Lee-Dadswell, B. G. Nickel, and C. G. Gray, Phys. Rev. E **72**, 031202 (2005).
 - [23] G. R. Lee-Dadswell, B. G. Nickel, and C. G. Gray, J. Stat. Phys. **132**, 1 (2008).
 - [24] G. R. Lee-Dadswell, Phys. Rev. E **91**, 032102 (2015).
 - [25] P. I. Hurtado and P. L. Garrido, arXiv:1506.03234v1 (2015).
 - [26] Y. Zhong, Y. Zhang, J. Wang, and H. Zhao, Phys. Rev. E **85**, 060102(R) (2012).
 - [27] S. Chen, Y. Zhang, J. Wang, and H. Zhao, J. Stat. Mech. (2016) 033205.
 - [28] A. V. Savin and Y. A. Kosevich, Phys. Rev. E **89**, 032102 (2014).
 - [29] S. G. Das, A. Dhar, and O. Narayan, J. Stat. Phys. **154**, 204 (2014).
 - [30] L. Wang, B. Hu, and B. Li, Phys. Rev. E **88**, 052112 (2013).
 - [31] S. Chen, J. Wang, G. Casati, and G. Benenti, Phys. Rev. E **90**, 032134 (2014).
 - [32] D. SK. Sato, Phys. Rev. E **94**, 012115 (2016).
 - [33] J. Jiang and H. Zhao, arXiv:1603.04819 (2016).
 - [34] C. Giardiná, R. Livi, A. Politi, and M. Vassalli, Phys. Rev. Lett. **84**, 2144 (2000).
 - [35] O. V. Gendelman and A. V. Savin, Phys. Rev. Lett. **84**, 2381 (2000).
 - [36] S. G. Das and A. Dhar, arXiv:1411.5247v2 (2015).
 - [37] H. Spohn, arXiv:1411.3907v1 (2014).
 - [38] D. Roy, Phys. Rev. E **86**, 041102 (2012).
 - [39] D. Xiong, Europhys. Lett. **113**, 140002 (2016).
 - [40] D. Xiong, J. Stat. Mech.: Exp. Theor. (2016) 043208.
 - [41] H. Zhao, Phys. Rev. Lett. **96**, 140602 (2006).
 - [42] S. Chen, Y. Zhang, J. Wang, and H. Zhao, Phys. Rev. E **87**, 032153 (2013).
 - [43] A. Sarmiento, R. Reigada, A. H. Romero, and K. Lindenberg, Phys. Rev. E **60**, 5317 (1999).
 - [44] R. Reigada, A. H. Romero, A. Sarmiento, and K. Lindenberg, J. Chem. Phys. **111**, 1373 (1999).
 - [45] A. Sarmiento, A. H. Romero, J. M. Sancho, and K. Lindenberg, J. Chem. Phys. **112**, 10615 (2000).
 - [46] D. Forster, *Hydrodynamic Fluctuations, Broken Symmetry, and Correlation Functions* (Benjamin, New York, 1975).
 - [47] J. P. Hansen and I. R. McDonald, *Theory of Simple Liquids*, 3rd ed. (Academic, London, 2006).
 - [48] D. Xiong and E. Barkai, arXiv:1606.06402v3(2016).
 - [49] S. Denisov, V. Zaburdaev, and P. Hänggi, Phys. Rev. E **85**, 031148 (2012).
 - [50] A. Rebenshtok, S. Denisov, P. Hänggi, and E. Barkai, Phys. Rev. Lett. **112**, 110601 (2014).
 - [51] S. Denisov, J. Klafter, and M. Urbakh, Phys. Rev. Lett. **91**, 194301 (2003).
 - [52] B. Li and J. Wang, Phys. Rev. Lett. **91**, 044301 (2003).
 - [53] N. Li, B. Li, and S. Flach, Phys. Rev. Lett. **105**, 054102 (2010).